Irvy M.A.Gledhill[1], Hamed Roohani[2], Karl Forsberg[3], Peter Eliasson[3], Beric W. Skews[2] and Jan Nordström[4]

Theoretical treatment of fluid flow for accelerating bodies

[1] Aeronautical Systems Competency Area, Defence, Peace, Safety and Security Unit, CSIR, Pretoria, 0001, South Africa
[2] School of Mechanical, Aeronautical and Industrial Engineering, University of the Witwatersrand, Johannesburg, 2050, South Africa
[3] FOI, Totalförsvarets forskningsinstitut, The Swedish Defence Research Agency, 164 90, Stockholm, Sweden
[4] Division of Computational Mathematics, Department of Mathematics, Linköping University, SE-581 83, Linköping, Sweden
Corresponding author:
Prof. I.M.A. Gledhill
DPSS
CSIR
PO Box 395
Pretoria 0001
South Africa
Email (preferred): igledhil@csir.co.za
Telephone: +27 12 841 2769
Mobile: +27 82 4139134
Fax: +27 12 349 1156

Accepted by Theoretical and Computational Fluid Dynamics, Springer 05/02/2016
DOI: 10.1007/s00162-016-0382-0

Abstract Most computational fluid dynamics simulations are, at present, performed in a body-fixed frame, for aeronautical purposes. With the advent of sharp manoeuvre, which may lead to transient effects originating in the acceleration of the centre of mass, there is a need to have a consistent formulation of the Navier-Stokes equations in an arbitrarily moving frame. These expressions should be in a form that allows terms to be transformed between non-inertial and inertial frames, and includes gravity, viscous terms, and linear and angular acceleration. Since no effects of body acceleration appear in the inertial frame Navier-Stokes equations themselves, but only in their boundary conditions, it is useful to investigate acceleration source terms in the non-inertial frame. In this paper, a derivation of the energy equation is provided in addition to the continuity and momentum equations previously published. Relevant dimensionless constants are derived which can be used to obtain an indication of the relative significance of acceleration effects. The necessity for using Computational Fluid Dynamics to capture non-linear effects remains, and various implementation schemes for accelerating bodies are discussed. This theoretical treatment is intended to provide a foundation for interpretation of aerodynamic effects observed in manoeuvre, particularly for accelerating missiles.

Keywords fluid physics · Navier-Stokes equations · arbitrary acceleration · manoeuvre · Computational Fluid Dynamics · non-inertial frame

1 Introduction

Current aircraft and missile systems place increased reliance on high agility. Fifth generation missiles turn at a maximum lateral acceleration of 60g to 100g, where g is the acceleration due to gravity. Projectiles may be subjected to thrust of the order of 100g to 500g at launch, and thrust vectoring is commonly used for air-to-air missiles. As a result, there is an increasing need for a consistent set of Navier-Stokes equations in arbitrarily moving frames as a basis for further development in the field of accelerating aerodynamics, specifically to assist in understanding the dynamics of manoeuvring air vehicles in conjunction with CFD. The set of equations should cover subsonic, transonic, and supersonic regimes, and provide insight on the physics of fluids in accelerating frames. It should define scalar, vector and tensor properties in inertial and non-inertial frames, and show clearly which coordinate systems are being used in either. The equations should include both viscous and gravitational terms as well as linear or turning acceleration. In this paper the energy equation for arbitrary acceleration in general non-inertial frames of reference is presented, based on the work of Löfgren (unpublished reports FFAP-A-1040 and FFAP-B-066, The Aeronautical Research Institute of Sweden, 1995 and 1998 respectively) and Forsberg (unpublished report, The Aeronautical Research Institute of Sweden, 1998) and following the continuity and momentum conservation equations previously formulated by Gledhill *et al*. [1]. From the accelerating frame formulation, a set of dimensionless constants is derived, which, under specified circumstances, can be used to determine whether acceleration effects are likely to be significant in a specified regime of interest in terms of the relative importance of linear terms.

To date, most aeronautical design, and guidance and control, has been based on steady-state analysis, supplemented by dynamic derivatives, with the notable exception of aeroelastic configurations. However, an increasing number of applications now require an understanding, not simply of transient effects, but of the aerodynamics of significantly accelerating objects. The examples of interest for this paper are rapidly manoeuvring missiles, missiles under significant unidirectional acceleration, and projectiles experiencing spin-down or spin-up. In these cases, flow changes are observed over a trajectory which is orders of magnitude longer than the vehicle itself.

Added mass effects are important for manoeuvre for vehicles suspended in a medium of similar density to their own, such as airships and submarines. In some of these cases, the vehicle is moving within its own wake, and the flow effects are important within a domain of the same order of size as the vehicle itself. In the present work, the emphasis is on arbitrary manoeuvre over a path that is longer than the typical length of the vehicle, although the theory can be applied when it is relevant to local effects such as periodic motions, aeroelastic motions, rotors, oscillating wings, or effects which can be modelled as locally unsteady without considering acceleration of the centre of mass of the vehicle.

This paper is intended to set out the relevant fundamental theory in a form useful for finite-volume implementation. For that reason, illustrations have been given in terms of examples that have already been published by our group and others. The restricted case of acceleration along a straight line is described, and dimensionless parameters for example configurations are illustrated.

2 Earlier work

Turbine engine design, and geophysical flows, have been the primary fields in which rotating flow has been of interest, and formulations of equations for constant angular velocity flow are to be found in fundamental textbooks [2,3]. The theory of rotating fluids was explored by Hough [4], Proudman [5], Taylor [6,7] and Boubnov and Golitsyn [8], and is summarised by Greenspan [9] and Owczarek [10], using derivations based on flow volumes in contrast to the current general transforms.

Several early authors performed analytical studies of Stokes flow over bodies accelerating in incompressible viscous flow at low Reynolds numbers, deriving the force on a sphere and an expression for the boundary layer. This led to the formulation of the Basset-Bousinessq-Oseen equation for the motion of a particle in the limit of low Mach and Reynolds numbers and its subsequent extension to compressible flow [11]. The terms Bousinessq-Basset force, Basset force [12] or history force refer to the fact that the development of a boundary layer over an accelerating particle in a fluid depends on the temporal history of the fluid near the particle surface. Boundary layer start-up processes with impulsive or finite acceleration were studied analytically by Blasius [13], Görtler [14] and Schlichting [15], and similar studies have been performed for spheres and spinning spheres [16,17,18] for constant acceleration or falling under gravity. Renewed interest in boundary layers with accelerating or decelerating free-stream flow (as in a converging flow) has led to many studies, *e.g.* [19,20,21], of flow within favourable pressure gradients, and of relaminarisation. This work is relevant to understanding the behaviour of turbulent boundary layers at accelerating walls if acceleration effects are small enough for Galilean invariance to be assumed.

The requirement for an understanding of noise from supersonic aircraft prompted a geometrical analysis of Mach and shock waves, supported by towing-tank experiments, by Lilley *et al.* [22].

A potentially useful direction in terms of simulation is that of deriving invariant schemes for moving frames based on numerical considerations, and is largely based on the work of Olver [23] involving Lie group transformations of partial differential equations. Poludnenko and Khokhlov [24] required a simulation system for astrophysics and cosmology which would be suitable for cases where the typical flow speeds are very much larger than the sound speed or the local flow velocities, in, for example, stellar cores or galactic formation. The inviscid equations are derived using a transformation into a non-inertial rotating frame with scaling factors in time, space, and density for this purpose. The computational frame transform is chosen to be reasonably close to the expected stellar or galactic evolution, including oscillatory motions. In a similar way Chhay and Hamdouni [25] derived symmetrisation parameters for the inviscid flow equation transformation groups. These methods are particularly useful when expansion and contraction is very significant rather than centre of mass acceleration.

Understanding of added mass effects has also depended on the history force concept [26] and has been reviewed and measured in low Reynolds number experiments with gravitational acceleration [27]. A drag calculation for a manoeuvring underwater vehicle was worked out from first principles by Sonowski *et al.* [28] for use in a navigation, object detection and collision avoidance system, and performed well in a simulated environment.

In terms of dimensionless numbers which may aid in defining flow regimes, work from the area of tunnel startup by Freymuth *et al.* [29], two useful dimensionless parameters were introduced: a dimensionless time, $t^* = \frac{t}{\sqrt{a/L}}$, where L is a typical length and the normalising time is the typical time for air to cross length L from rest at constant acceleration a; and a Reynolds number in acceleration, $R = \frac{L\sqrt{La}}{\nu}$, based on the final velocity after acceleration from rest, and the kinematic viscosity ν.

Given the need for prediction of loads on manoeuvring missiles, Löfgren (*ibid.*) developed a mathematical toolbox for arbitrarily moving frames of reference. This study was initiated with the derivation of the properties of general linear transforms between arbitrarily moving frames, with relative motion defined by functions of continuous differentiability of class C^2, in $\mathbb{R}^{n+1}$ spaces with n spatial dimensions. Transformations for scalars, vectors and tensors, and operators, were defined, from which transforms of derivatives were deduced. General conservation equations were written for moving volumes, and then reduced to three spatial dimensions. The equations for particle motion, and for fluid conservation, could then be written. The weak variants of the differential equations of fluid flow were examined assuming local differentiability in the solutions, and jump conditions at discontinuities were derived. The integral forms of the conservation equations were derived for moving control volumes. Any two arbitrarily moving frames were treated to this point in a symmetrical way, and from these results conservation relations for mass, momentum and energy were derived specifically for inertial and non-inertial frames. Forsberg (*ibid.*) then formulated the mass, momentum and energy conservation equations in preparation for CFD implementation. Forsberg's derivation of the

mass and momentum conservation relations appeared in 2003 [30] together with CFD implementation and applications. The concept of generalised rothalpy was introduced by Forsberg, and is provided here, together with Forsberg's derivation of the energy equation, which is now extended to include external forces in order to demonstrate the relationship between gravitational effects and the effects of an arbitrarily accelerating frame origin.

Gledhill *et al.* [1] published the continuity and momentum equations and demonstrated an implementation in the code EURANUS [31], by performing the computations in the inertial frame. This approach has the considerable advantages of (1) a very simple development path from an existing moving-mesh model with spatial conservation [31], in which boundary conditions are the main modifications required, and (2) the fact that the source terms appearing in the relative frame model (below) do not need to be discretised, implemented, verified or validated. It is known that source terms such as those required for acceleration can make the numerical system stiff.

Limache [32,33] approached the problem using the methodology of Owczarek [10] specifically for aerodynamically steady motions, motivated by the potential for using these as a set of characteristic motions for the description of general manoeuvre. The Navier-Stokes equations were generalised for aerodynamically steady flow, and non-dimensionalised so that coefficients could be written in terms of Reynolds, Prandtl and Mach numbers. Non-dimensional coefficients were not, however, explored for characterisation of the significance of acceleration. A method of derivation of the Coriolis effect in the momentum equation has been described by Kageyama and Hyodo [34], using Galilean transformation between successive inertial frames. The method ultimately leads to a momentum equation equivalent to those derived by Batchelor and Greenspan [3,9]. Gardi [35] presented similar momentum and energy terms as source terms for a non-inertial moving reference frame and discussed discretisation errors in comparison with an Arbitrary-Lagrangian-Eulerian approach. Combrinck and Dala [36] extended the procedure of Kageyama and Hyodo [34] to transforming the Navier-Stokes equations under pure rotation, for constant and varying angular velocity, using successive transforms between an inertial frame, an orientation preserving frame, and a rotated frame. The two moving frames have the same angular velocity. It was demonstrated that internal energy conservation is invariant. The results are shown for compressible and incompressible flow.

The work in this paper extends the theoretical endeavour described above to expressions for generalised rothalpy, the derivation of dimensionless constants specifically for the purpose of characterising regimes in accelerating flight, and the illustration of these parameters for practical cases.

CFD calculations on accelerating aerofoils or missiles have been carried out by very few authors. Inoue *et al.* [37] used an early simulation in the inertial frame to simulate a constant speed diamond aerofoil describing a parabolic path, for the purpose of investigating shock focussing within the arc. Forsberg *et al.* [30] and Gledhill *et al*. [1] provided the basis of the theory for the continuity and momentum equations as given here, validated an implementation in the inertial frame within the finite-volume code EURANUS using the oscillating aerofoil data of Landon [38], and then used a model of the NACA0012 aerofoil on constant pitch trajectories [39] to illustrate the necessity for inclusion of acceleration effects in the calculation of pitch damping. It was then demonstrated that drag on an axisymmetric flare missile dropped by 20% in comparison with steady values if the flare geometry was accelerated through the transonic range at 4 500 ms^{-1}.

Roohani and Skews have conducted detailed studies of the unsteady aerodynamics of accelerating bodies, such as aerofoils [40-44] and axisymmetric objects [45] undergoing unidirectional acceleration through the subsonic and transonic ranges. This was modelled numerically using source terms added to the momentum and energy equations in the code FLUENT [46].Shock wave boundary layer interaction was found to have significant effect on the shock wave position and strength in the transonic range. Comparison of lift, pitching moment, and drag, as well as shock and flow field behaviour in acceleration, deceleration and steady state at specific Mach numbers during flight revealed significant differences between the steady and unsteady scenarios. Acceleration dependent behaviour for bow shocks, tail shocks and trailing compression waves were observed. In conclusion, all differences between steady and unsteady transonic shock wave behaviour and lift were found to be predominantly a function of flow history, while differences between steady and unsteady subsonic drag were mainly due to fluid inertia. It was shown that the angle at which separation occurs at a specific subsonic Mach number varies between the steady, accelerating and decelerating scenarios [47].

At this point it is important to explain the concept of flow history as used in the present context [43]. When an object is accelerated in a compressible fluid, the unsteady flow field generated is not allowed sufficient time to reach equilibrium at any specific Mach number. It is therefore different from the steady state flow field at that same Mach number and is in fact influenced by its own earlier flow field characteristics. During acceleration, subsonic lift values are found to be lower than the corresponding steady state values at the same Mach number because the unsteady flow field has

insufficient time to reach equilibrium and will reflect some of the earlier characteristics when the Mach number was lower.

In terms of significant angular velocity, the findings of Naidoo and Skews [48,49] for the flow field about a rapidly accelerating wedge causing shock reflection off a wall showed hysteresis effects in transition between regular and Mach reflection. These effects take place within a local domain, and accurate observations from wind tunnel experiments were made and compared with moving-mesh CFD.

Experimental data for validation purposes is rare for long trajectories, but ballistic ranges can provide some data. The application of CFD to prediction of the characteristics of army projectiles was initiated at Aberdeen Proving Ground for calculations of pitch damping force and moment coefficients [50,51]. As a method of computing flow fields in deceleration for comparison with ballistic range data, Saito *et al.* [52] used an inertial frame CFD system for models of shock stand-off distance.

In practical aeronautical terms, since it is of considerable importance to predict dynamic derivatives for missiles and projectiles, and to some extent these needs have driven the field of manoeuvre modelling forward [53,54,55]. Sturek *et al.* [56], Wienacht [51], Murman *et al.* [57], and McIlwain *et al.* [58] have employed prescribed-trajectory methods for missiles in local domains. The coupling of time-accurate CFD with rigid body dynamics allows the prediction of trajectories, but computational resources are not yet sufficient to make this viable for more than fractions of a second [59]. The use of flight dynamic databases through which a configuration is "flown" has been developed in aircraft manoeuvre modelling, and for complex non-linear manoeuvres requires the addition of dynamic derivatives [60] and, as a next step, Reduced-Order Methods (*e.g.* [61]). These have proved reasonable for linear coefficients, but less accurate for non-linear rolling and yawing moments.

Given the above, there is a need for a theoretical basis and a complete set of conservation equations in both inertial and non-inertial frames on which further work can be founded, particularly for manoeuvre over extended trajectories. Transformation of the continuity and momentum equations [1] is extended here to the energy equation. Part of the motivation for developing this theory is to develop guidance about what constitutes "significant" acceleration, and how the regimes of flow about accelerating objects can be distinguished and quantified. As a step in this direction, some dimensionless constants are derived. Where data is available, these constants have been calculated, and some remarks about their applicability are made. A further reason for presenting the theory is to assist in supporting decisions about the relative merits of numerical models in inertial and non-inertial frames.

The approach presented here is given in terms of familiar formulations of the conservation equations that are frequently used in aerospace applications. The distinctions between expression of these equations in inertial and non-inertial frames is clearly made. The theory given here has the advantages of allowing transformation between body-fixed coordinates attached to manoeuvring vehicles, and inertial frames, in which flow fields and flow phenomena are often unfamiliar and harder to interpret. Many of the source terms arising in the momentum equation are familiar, and are given here in a general and inclusive way for all the effects of arbitrary trajectories. The energy equation is presented in a form from which cross-terms can be identified, and, in future, quantified.

3 Theory

A mathematical toolbox for the treatment of non-stationary problems with moving boundaries, for application in fluid dynamics and aeronautics, was formulated by Löfgren (*ibid.*). Löfgren developed an algebraic basis for a finite-dimensional vector space, in which linear transformations relevant to fluid balance equations could be defined. Space and time were treated on an equal footing as far as possible. The properties of functions and derivatives under transformation were developed, and the conservation equations were constructed in arbitrarily moving control volumes. The conservation laws were expressed in terms of displacement vectors $\boldsymbol{x}$ and time t, for density $\rho = \rho(\boldsymbol{x}, t)$, velocity $\boldsymbol{v} = \boldsymbol{v}(\boldsymbol{x}, t)$, pressure $p = p(\boldsymbol{x}, t)$, temperature $T = T(\boldsymbol{x}, t)$, and an external force per unit mass $\boldsymbol{g} = \boldsymbol{g}(\boldsymbol{x}, t)$, in two arbitrarily moving frames of reference Σ and Σ'. A generalised conservation equation in its strong integral form was treated for an arbitrarily moving volume, and the weak differential form was developed. One of the frames was then constrained to be an inertial frame, in which Newton's Laws hold, and are expressed in the form of conservation equations. The transforms to the arbitrarily moving frame Σ' were derived for two dynamic systems: for a finite mass particle, and for a homogeneous fluid. Löfgren was able to prove the hypothesis that "for a fluid in space, the same balance equations hold in Σ' as in Σ, provided that in Σ' we add the inertial terms per mass unit which would be added in the case of a particle".

This work established a sound mathematical foundation for the expression of the method in a form suitable for making choices between possible numerical implementations in an inertial frame or in non-inertial frames by Forsberg (*ibid.*), which forms the basis for the analysis given here.

In Forsberg's formulation, vectors are expressed in an inertial frame and in an arbitrarily moving frame. Since the latter may also be an inertial frame if it moves with constant velocity relative to the inertial frame, we sometimes refer to it as the *relative* frame, and to the inertial frame as the *absolute* frame.

Any convenient inertial frame may be chosen as the absolute frame Σ. For aeronautical purposes, it has been useful to illustrate the inertial frame as being fixed to "the ground". This frame is not in fact inertial, since it is rotating and moving with the earth, and is in a gravitational field. The inertial frame in our analysis can be defined as being stationary with respect to an infinite domain of still air, and gravity is accommodated as a body force in the equations of motion without loss of generality.

The relative frame Σ' may be chosen as, for example, fixed to a manoeuvring missile in such a way that the orientation of the body axes follows that of the object. CFD has usually been carried out on a mesh in this frame, and for this reason, flow fields about objects have traditionally been interpreted in this frame. In the relative frame Σ', a stagnation point with zero velocity relative to the missile appears at the leading edge or nose, and non-zero values of the velocity are specified at the far-field boundaries of the finite domain mesh. In contrast, if the flow is simulated by a mesh attached to the object moving through the absolute frame and computations are performed in the absolute frame, the far-field boundaries of the moving mesh encounter stagnant air, and therefore the far-field boundary condition on each velocity component is zero. The wall at the leading edge of the flying object is travelling with a non-zero time-dependent velocity. The velocity boundary conditions of the missile wall are determined by the dynamics of the flight, and the velocity of air in close proximity to the leading edge will be non-zero. Near solid non-slip walls in viscous flow, the boundary layer will exhibit velocities in the viscous sublayer close to those determined by the moving wall dynamics.

Once practical models are introduced, it is useful to provide a general transform between frames for ease of interpretation of familiar flow features, and for identification of new ones. This transformation gives rise to the phrases "as seen from the absolute frame" or "as seen from the relative frame" below. These refer to vector components with respect to a set of orthonormal basis vectors $\{e_1, e_2, e_3\}$ or $\{e_1', e_2', e_3'\}$.

3.1 Notation and transforms

Consider an inertial frame Σ (Figure 1(a)) and a non-inertial frame Σ' (Figure 1(b)). We establish the following notation for vectors and tensors in these frames:

$\boldsymbol{a}$ is a vector in Σ described by coordinates in Σ,
$\breve{\boldsymbol{a}}$ is a vector in Σ described by coordinates in Σ',
$\underline{\boldsymbol{a}}$ is a vector in Σ' described by coordinates in Σ', and
$\underline{\hat{\boldsymbol{a}}}$ is a vector in Σ' described by coordinates in Σ.

In summary, the underscore notation describes a vector in the relative frame, while the breve ($\breve{}$) and circumflex ($\hat{}$) are used to indicate transformed vectors. As an example, the components of gravity vector $\boldsymbol{g}$ expressed with respect to a set of basis vectors in Σ are constant in time, but if Σ' rotates, the equivalent vector $\breve{\boldsymbol{g}}$ expressed in terms of a basis set in Σ' will have time-dependent components. The mapping between Σ and Σ' back is defined by a unitary transform U defined in the following way:

$$\underline{\hat{\boldsymbol{a}}} = \boldsymbol{U} \cdot \underline{\boldsymbol{a}} \tag{1}$$

Then

$$\breve{\boldsymbol{a}} = \boldsymbol{U}^{-1} \cdot \boldsymbol{a} = \boldsymbol{U}^{t} \cdot \boldsymbol{a} \tag{2}$$

$$\underline{\breve{\boldsymbol{a}}} = \underline{\boldsymbol{a}} \tag{3}$$

and

$$\det(\boldsymbol{U}) = 1. \tag{4}$$

Here $\boldsymbol{U}$ may be interpreted as a rotation such as

$$\boldsymbol{U} = \begin{bmatrix} cos\theta & -sin\theta & 0 \\ sin\theta & cos\theta & 0 \\ 0 & 0 & 1 \end{bmatrix} \tag{5}$$

where θ is an axis angle, in this case with respect to e_3. Tensors are transformed by

$$\breve{\boldsymbol{\tau}} = \boldsymbol{U^t} \cdot \boldsymbol{\tau} \cdot \boldsymbol{U}, \boldsymbol{\tau} = \boldsymbol{U} \cdot \breve{\boldsymbol{\tau}} \cdot \boldsymbol{U^t} \tag{6}$$

We now need to relate position vectors in the two frames. A position vector in the inertial frame is denoted by $\boldsymbol{x}$, and we define the transform relating $\underline{\boldsymbol{x}}$ in the relative frame to $\boldsymbol{x}$ by

$$\boldsymbol{x} = \boldsymbol{r} + \boldsymbol{U} \cdot \underline{\boldsymbol{x}} \text{ and } \underline{\boldsymbol{x}} = \underline{\boldsymbol{r}} + \boldsymbol{U^t} \cdot \boldsymbol{x}. \tag{7}$$

Here $\boldsymbol{r}(t)$ is the position vector of O', the origin of Σ', relative to O, the origin of Σ. As an example, $\underline{\boldsymbol{x}}$ may denote a position vector of a point P relative to body axes with origin O' fixed in the body, and $\boldsymbol{x}$ is the position vector of P with respect to O. We note for $\underline{\boldsymbol{x}} = 0$ that $\underline{\boldsymbol{r}} = -\boldsymbol{U^t} \cdot \boldsymbol{r}$ and $\boldsymbol{r} = -\boldsymbol{U} \cdot \underline{\boldsymbol{r}}$. For acceleration cases we require that $\boldsymbol{r}(t)$ is C^2 regular in time, *i.e.* that the second derivative with respect to time is continuous and smooth. Note that $\boldsymbol{r}$ may be used to describe revolution of O'about O, while $\boldsymbol{U}$ and $\boldsymbol{\omega}$ (below) describe spin or rotation about O'. The two angular displacements and velocities need not be the same.

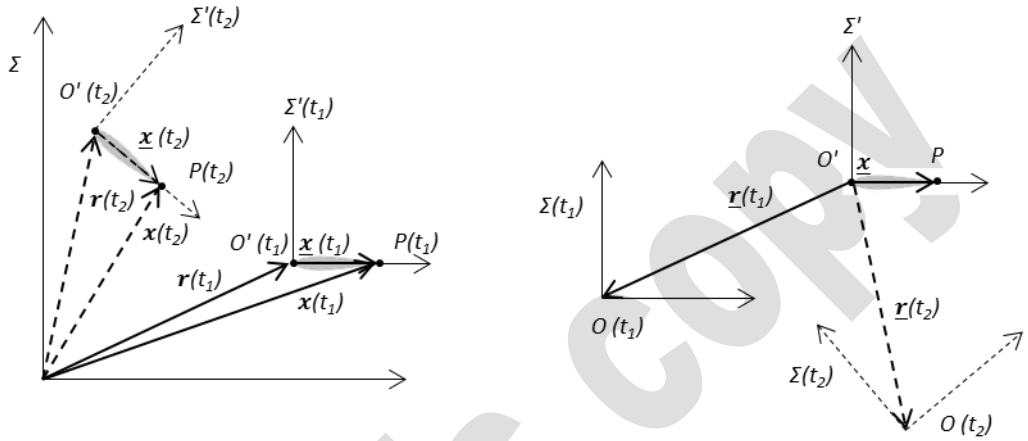

(a) **(b)**

Figure 1 (a) Position vectors seen from Σ at successive times t_1 and t_2, **(b)** Position vectors seen from Σ' at successive times t_1 and t_2

For time derivatives it is convenient to define a vector $\boldsymbol{\omega}$ by

$$\boldsymbol{\omega} \times \left(\boldsymbol{U} \cdot \underline{\boldsymbol{a}}\right) = \frac{\partial \boldsymbol{U}}{\partial t} \cdot \underline{\boldsymbol{a}} \tag{8}$$

Differentiating with respect to time (and using dot notation for time derivatives) we obtain absolute and relative velocities respectively:

$$\begin{aligned} \boldsymbol{v} = \frac{d\boldsymbol{x}}{dt} &= \frac{d\boldsymbol{r}}{dt} + \frac{\partial}{\partial t}\boldsymbol{U} \cdot \underline{\boldsymbol{x}} \\ &= \dot{\boldsymbol{r}} + \boldsymbol{U} \cdot \left(\breve{\boldsymbol{\omega}} \times \underline{\boldsymbol{x}} + \underline{\boldsymbol{v}}\right) \qquad (9) \\ &= \dot{\boldsymbol{r}} + \widehat{\underline{\boldsymbol{v}}} + \boldsymbol{\omega} \times \widehat{\underline{\boldsymbol{x}}} \qquad (10) \end{aligned}$$

Similarly

$$\underline{\boldsymbol{v}} = -\dot{\boldsymbol{r}} + \breve{\boldsymbol{v}} - \breve{\boldsymbol{\omega}} \times \boldsymbol{x}. \tag{11}$$

An inter-frame or system point velocity field $\underline{\boldsymbol{u}}$ between the two frames is defined by

$$\underline{\boldsymbol{u}} = \breve{\boldsymbol{v}} - \underline{\boldsymbol{v}} \tag{12}$$

which leads to an interframe acceleration term

$$\dot{\underline{\boldsymbol{u}}} = \dot{\breve{\boldsymbol{r}}} + \dot{\breve{\boldsymbol{\omega}}} \times \underline{\boldsymbol{x}} \tag{13}$$

where × denotes a vector cross product. We can also show for a general vector a that

$$\boldsymbol{a} \cdot \boldsymbol{\nabla}\underline{\boldsymbol{u}} = \breve{\boldsymbol{\omega}} \times \boldsymbol{a}. \tag{14}$$

3.2 Conservation equations

We are interested in deriving conservation laws expressed in Σ' for several purposes. The first is that a number of effects in a non-inertial frame are familiar, such as the Coriolis effect, and should be shown in the context of flow around accelerating bodies; the second is that terms for linear acceleration and angular acceleration in rotation and revolution should be identifiable; and the third is to illustrate the use of dimensionless parameters in this field. In a previous paper, the derivation of the conservation

equations for mass and momentum was presented by Gledhill *et al.* [1]. In the following paragraphs, the mass and momentum equations are summarised, and the energy equation is derived.

The aim is to start with the conservation equations in Σ, expressed in terms of $\boldsymbol{v}$, and write them in terms of $\underline{\boldsymbol{u}}$ and $\underline{\boldsymbol{v}}$, the velocity in Σ′ with respect to coordinates in Σ′. In the latter form, without any acceleration, they correspond to the solution commonly used in external CFD. Without acceleration, both frames are inertial, and the equations take the same form for $\boldsymbol{v}$ and Σ as they do for $\underline{\boldsymbol{v}}$ and Σ′.The intrinsic functions ρ, p, e and T are Galilean invariant and undergo a change of variables. Since $\underline{\boldsymbol{r}}$ is easy to transform, $\breve{\boldsymbol{r}}$ may be used. Some parameters, such as the stress tensor, $\boldsymbol{\tau}$, are not the focus of the current development, but the fact that they are written in terms of coordinates in Σ′, *e.g.* $\breve{\boldsymbol{\tau}}$ **,** allows the form in which they have been included to be clearly identified for further expansion.

3.3 General conservation laws

Mappings $\phi: \mathbb{R}^{1+3} \to \mathbb{R}^{1+3}$ defined by $\varphi(t, \underline{\boldsymbol{x}}) = (t, \boldsymbol{r} + \boldsymbol{U} \cdot \boldsymbol{x})$, and the inverse $\varphi^*(t, \boldsymbol{x}) = (t, -\breve{\boldsymbol{r}} + \boldsymbol{U^t} \cdot \underline{\boldsymbol{x}})$, are performed. Then conservation equations may be written in the absolute frame Σ in strong form as follows, where the symbol $\boldsymbol{a}$ may represent a scalar (an element of $\mathbb{R}^1$), or a vector (an element of $\mathbb{R}^3$), for a moving volume V:

$$\frac{\partial}{\partial t}\int_V \rho \boldsymbol{a} dV + \oint_{\partial V} (\rho \boldsymbol{a} \underline{\hat{\boldsymbol{v}}} + \boldsymbol{F}_a) \cdot d\underline{\hat{\boldsymbol{S}}} = \int_V Q_a dV \tag{15}$$

where Q_a is the volume source term of $\boldsymbol{a}$, $\boldsymbol{F}_a$ is a flux term, and $d\boldsymbol{S}$ are surface normals, which can be defined in a natural way in the reference frame as $d\underline{\hat{\boldsymbol{S}}}$. The volume element dV is conserved across frames by the definition of $\boldsymbol{U}$. To express this equation in the relative frame Σ′, the mapping φ^* is applied:

$$\tfrac{\partial}{\partial t}\textstyle\int_V\ \phi^*(\rho \boldsymbol{a}) dV + \oint_{\partial V} (\phi^*(\rho \boldsymbol{a} \underline{\hat{\boldsymbol{v}}}) + \phi^* \boldsymbol{F}_a) \cdot d\underline{\boldsymbol{S}} = \textstyle\int_V\ \phi^* Q_a dV. \tag{16}$$

The functions ρ, p, T and Q_a can be treated as scalar functions with the change of variable specified by φ^*. Then

$$\tfrac{\partial}{\partial t}\textstyle\int_V\ \phi^*(\rho \boldsymbol{a}) dV + \oint_{\partial V} [\phi^*(\rho \boldsymbol{a})(\phi^* \boldsymbol{v} - \underline{\boldsymbol{u}}) + \phi^* \boldsymbol{F}_a] \cdot d\underline{\boldsymbol{S}} = \textstyle\int_V\ \phi^* Q_a dV. \tag{17}$$

Now it is possible to regard the scalar functions as defined in Σ′ and omit ϕ^* for convenience to write, in Σ′,

$$\frac{\partial}{\partial t}\int_V \rho \boldsymbol{a} dV + \oint_{\partial V} (\rho \boldsymbol{a} \underline{\boldsymbol{v}} + \breve{\boldsymbol{F}}_a) \cdot \boldsymbol{d}\underline{\boldsymbol{S}} = \int_V Q_a dV \tag{18}$$

Using Green's theorem, the differential form in the relative frame can be written

$$\frac{\partial}{\partial t}(\rho \boldsymbol{a}) + \boldsymbol{\nabla} \cdot \left(\rho \boldsymbol{a} \underline{\boldsymbol{v}} + \breve{\boldsymbol{F}}_a\right) = Q_a \tag{19}$$

Alternatively, equation (19) can be proved by writing the forms of derivatives under φ^*.

3.4 Conservation of mass

The mass continuity equation is obtained with scalar $a = 1$, $\boldsymbol{F}_a = 0$ and $Q_a = 0$ in the absence of sources or sinks. In the absolute frame:

$$\frac{\partial}{\partial t}\int_V \rho dV + \oint_{\partial V} \rho \underline{\hat{\boldsymbol{v}}} \cdot d\underline{\hat{\boldsymbol{S}}} = 0 \tag{20}$$

or equivalently in the relative frame

$$\frac{\partial}{\partial t}\int_V \rho dV + \oint_{\partial V} \rho \underline{\boldsymbol{v}} \cdot \boldsymbol{d}\underline{\boldsymbol{S}} = 0 \tag{21}$$

or

$$\frac{\partial \rho}{\partial t} + \boldsymbol{\nabla} \cdot \left(\rho \underline{\boldsymbol{v}}\right) = 0. \tag{22}$$

3.5 Conservation of momentum

For the momentum conservation equation, $\boldsymbol{a} = \boldsymbol{v}$ in the inertial frame, $\boldsymbol{F}_a = p\boldsymbol{I} - \boldsymbol{\tau}$, where $\boldsymbol{I}$ is the identity matrix of rank three, and $Q_a = \rho \boldsymbol{g}$ in the absence of other external forces [2]:

$$\frac{\partial}{\partial t}\int_V \rho\boldsymbol{v}dV + \oint_{\partial V}(\rho\boldsymbol{v}\otimes\boldsymbol{v} + p\boldsymbol{I} - \boldsymbol{\tau})\cdot\boldsymbol{d\underline{\hat{S}}} = \int_V \rho\boldsymbol{g}dV \tag{23}$$

An outer product of tensors is required here. For a tensor Θ, with components $\theta_{i_{1\ldots n}}$, outer products are defined by $[\Theta\otimes\Psi]_{i_1\ldots i_n,j_1\ldots j_m} = \theta_{i_1\ldots i_n}\psi_{\ j_1\ldots j_m}$ and $U\cdot(\Theta\otimes\Psi) = (U\cdot\Theta)\otimes(U\cdot\Psi)$. To transform to the relative frame, it is therefore possible to write

$$\frac{\partial}{\partial t}\int_V \rho\breve{\boldsymbol{v}}dV + \oint_{\partial V}\left(\rho\breve{\boldsymbol{v}}\otimes\underline{\boldsymbol{v}} + p\boldsymbol{I} - \breve{\boldsymbol{\tau}}\right)\cdot\boldsymbol{d\underline{S}} = -\int_V (\rho\breve{\boldsymbol{\omega}}\times\breve{\boldsymbol{v}} - \rho\breve{\boldsymbol{g}})dV. \tag{24}$$

To express this in differential form we note that, owing to the definitions of scalar products and divergence operators $[\boldsymbol{\Theta}\cdot\boldsymbol{\Psi}]_{i_1\ldots i_{n-1},j_2\ldots j_m} = \sum_k \Theta_{i_1\ldots i_{n-1}k}\Psi_{k,j_2\ldots j_m}$ and $[\boldsymbol{\nabla}\cdot\boldsymbol{\Theta}]_{i_2\ldots i_n} = \sum_k \frac{\partial\Theta_{ki_2\ldots i_n}}{\partial x_k}$, it is correct to write

$$\oint_{\partial V}(\breve{\boldsymbol{v}}\otimes\underline{\boldsymbol{v}})\cdot d\underline{\boldsymbol{S}} = \int_V \nabla\cdot(\underline{\boldsymbol{v}}\otimes\breve{\boldsymbol{v}})dV$$

and therefore

$$\frac{\partial}{\partial t}(\rho\breve{\boldsymbol{v}}) + \boldsymbol{\nabla}\cdot\left(\rho\underline{\boldsymbol{v}}\otimes\breve{\boldsymbol{v}} + p\boldsymbol{I} - \breve{\boldsymbol{\tau}}\right) = -\rho\breve{\boldsymbol{\omega}}\times\breve{\boldsymbol{v}} + \rho\breve{\boldsymbol{g}}. \tag{25}$$

Note that in a rotating frame, the gravity vector $\breve{\boldsymbol{g}}$ will rotate. Using the method of Forsberg (*ibid.*) and Gledhill *et al.* [1] to write the expression in terms velocities $\breve{\boldsymbol{v}}$ expressed in Σ', (22) becomes

$$\begin{aligned}\frac{\partial}{\partial t}\int_V \rho\underline{\boldsymbol{v}}dV + \oint_{\partial V}\left(\rho\underline{\boldsymbol{v}}\otimes\underline{\boldsymbol{v}} + p\boldsymbol{I} - \breve{\boldsymbol{\tau}}\right)\cdot d\underline{\boldsymbol{S}} &= -\int_V \rho\left(\dot{\underline{\boldsymbol{u}}} + 2\breve{\boldsymbol{\omega}}\times\breve{\boldsymbol{v}} + \breve{\boldsymbol{\omega}}\times\breve{\boldsymbol{u}} + \breve{\boldsymbol{g}}\right)dV \\ &= -\int_V \rho[\breve{\boldsymbol{\omega}}\times(\breve{\boldsymbol{\omega}}\times\underline{\boldsymbol{x}}) + 2\breve{\boldsymbol{\omega}}\times\underline{\boldsymbol{v}} + \frac{\partial\breve{\boldsymbol{\omega}}}{\partial t}\times\underline{\boldsymbol{x}} + \frac{\partial\breve{\boldsymbol{r}}}{\partial t} - \breve{\boldsymbol{g}}]dV.\end{aligned} \tag{26}$$

In the relative frame in differential form this is

$$\begin{aligned}\frac{\partial}{\partial t}(\rho\underline{\boldsymbol{v}}) + \boldsymbol{\nabla}\cdot\left[\rho\underline{\boldsymbol{v}}\otimes\underline{\boldsymbol{v}} + p\boldsymbol{I} - \breve{\boldsymbol{\tau}}\right] \\ = -\rho\breve{\boldsymbol{\omega}}\times\left(\breve{\boldsymbol{\omega}}\times\underline{\boldsymbol{x}}\right) - 2\rho\breve{\boldsymbol{\omega}}\times\underline{\boldsymbol{v}} - \rho\dot{\breve{\boldsymbol{\omega}}}\times\underline{\boldsymbol{x}} - \rho\ddot{\breve{\boldsymbol{r}}} + \rho\breve{\boldsymbol{g}}.\end{aligned} \tag{27}$$

The source terms on the right hand side are easily identified as fictitious effects [9,2,3]: respectively, they are the centrifugal effect, the Coriolis effect, the Euler term for spin-up or spin-down [1], and translational acceleration. The final term on the right hand side is the effect of a body force on the fluid, in this case gravity.

3.6 Conservation of energy

To apply the general conservation relation for energy, we define $\boldsymbol{a} = E$, the total energy per unit mass, and $\boldsymbol{F}_a = p\boldsymbol{v} - \boldsymbol{\tau}\cdot\boldsymbol{v} - \kappa\boldsymbol{\nabla}T$. We note from the work of Löfgren that ρ, p and T are transformed by ϕ^* as above, and $\breve{\boldsymbol{v}}$ and $\boldsymbol{\tau}$ are an inertial frame vector and tensor respectively, expressed in coordinates of the relative frame. The total energy per unit mass is related to the internal energy per unit mass by

$$E = e + \frac{\|v\|^2}{2}. \tag{28}$$

A heat source is included as q_H and gravity is again applied as an external force acting on the fluid in the control volume dV [2],

$$Q_a = q_H + \rho\boldsymbol{v}\cdot\boldsymbol{g}. \tag{29}$$

In the absolute frame

$$\frac{\partial}{\partial t}\int_V \rho E dV + \oint_{\partial V}(\rho E\underline{\hat{\boldsymbol{v}}} + p\boldsymbol{v} - \boldsymbol{\tau}\cdot\boldsymbol{v} - \kappa\boldsymbol{\nabla}T)\cdot\boldsymbol{d\underline{\hat{S}}} = \int_V (q_H + \rho\boldsymbol{g}\cdot\boldsymbol{v})dV \tag{30}$$

and in the relative frame

$$\frac{\partial}{\partial t}\int_V \rho E dV + \oint_{\partial V}(\rho E\underline{\boldsymbol{v}} + p\breve{\boldsymbol{v}} - \breve{\boldsymbol{\tau}}\cdot\breve{\boldsymbol{v}} - \kappa\boldsymbol{\nabla}T)\cdot\boldsymbol{d\underline{S}} = \int_V (q_H + \rho\breve{\boldsymbol{g}}\cdot\breve{\boldsymbol{v}})dV. \tag{31}$$

Expressed in terms of velocities $\underline{\boldsymbol{v}}$ in the relative frame on the left hand side, and using equation (12),

$$\begin{aligned}\frac{\partial}{\partial t}\int_V \rho E dV + \oint_{\partial V}(\rho E\underline{\boldsymbol{v}} + p\underline{\boldsymbol{v}} - \breve{\boldsymbol{\tau}}\cdot\underline{\boldsymbol{v}} + p\underline{\boldsymbol{u}} - \breve{\boldsymbol{\tau}}\cdot\underline{\boldsymbol{u}} - \kappa\boldsymbol{\nabla}T)\cdot d\underline{\boldsymbol{S}} \\ = \int_V (q_H + \rho\breve{\boldsymbol{v}}\cdot\breve{\boldsymbol{g}})dV.\end{aligned} \tag{32}$$

The formulation of a generalised rothalpy conservation expression is now pursued. To rewrite in terms of $\underline{\boldsymbol{v}}$, equation (12) is used and it is noted that since $\underline{\boldsymbol{u}} = \breve{\boldsymbol{r}} + \breve{\boldsymbol{\omega}} \times \underline{\boldsymbol{x}}$,

$$\breve{\boldsymbol{v}} \cdot \breve{\boldsymbol{g}} = \underline{\boldsymbol{v}} \cdot \breve{\boldsymbol{g}} + \breve{\boldsymbol{r}} \cdot \breve{\boldsymbol{g}} + (\breve{\boldsymbol{\omega}} \times \underline{\boldsymbol{x}}) \cdot \breve{\boldsymbol{g}} = \underline{\boldsymbol{v}} \cdot \breve{\boldsymbol{g}} + \breve{\boldsymbol{r}} \cdot \breve{\boldsymbol{g}} - \underline{\boldsymbol{x}} \cdot (\breve{\boldsymbol{\omega}} \times \breve{\boldsymbol{g}}). \tag{33}$$

To relate internal energy and velocity $\breve{\boldsymbol{v}}$ through rothalpy, the scalar product of the momentum conservation relation, equation (25), with the inter-frame velocity is formed:

$$\frac{\boldsymbol{\partial}}{\boldsymbol{\partial t}}(\rho\breve{\boldsymbol{v}}) \cdot \underline{\boldsymbol{u}} + \left\{\boldsymbol{\nabla} \cdot \left[\rho\underline{\boldsymbol{v}} \otimes \breve{\boldsymbol{v}} + p\boldsymbol{I} - \breve{\boldsymbol{\tau}}\right]\right\} \cdot \underline{\boldsymbol{u}} = -\rho(\breve{\boldsymbol{\omega}} \times \breve{\boldsymbol{v}}) \cdot \underline{\boldsymbol{u}} + \rho\breve{\boldsymbol{g}} \cdot \underline{\boldsymbol{u}} \tag{34}$$

Since

$$\tfrac{\partial}{\partial t}\left(\rho\breve{\boldsymbol{v}} \cdot \underline{\boldsymbol{u}}\right) = \left(\tfrac{\partial}{\partial t}\rho\breve{\boldsymbol{v}}\right) \cdot \underline{\boldsymbol{u}} + \rho\breve{\boldsymbol{v}} \cdot \dot{\underline{\boldsymbol{u}}}, \tag{35}$$

equation (34) becomes

$$\frac{\partial}{\partial t}\left(\rho\breve{\boldsymbol{v}} \cdot \underline{\boldsymbol{u}}\right) + \left\{\boldsymbol{\nabla} \cdot \left[\rho\underline{\boldsymbol{v}} \otimes \breve{\boldsymbol{v}} + p\boldsymbol{I} - \breve{\boldsymbol{\tau}}\right]\right\} \cdot \underline{\boldsymbol{u}} = -\rho(\breve{\boldsymbol{\omega}} \times \breve{\boldsymbol{v}}) \cdot \underline{\boldsymbol{u}} + \rho\breve{\boldsymbol{v}} \cdot \dot{\underline{\boldsymbol{u}}} + \rho\breve{\boldsymbol{g}} \cdot \underline{\boldsymbol{u}}. \tag{36}$$

Using the definition of the inter-frame velocity, it is not difficult to show that $\boldsymbol{\nabla}\underline{\boldsymbol{u}}$ is an anti-symmetric tensor, and that its inner product with any symmetric tensor is 0, the inner product being defined for second rank tensors as $\Theta : \Psi = \sum_{ij} \theta_{ij}\psi_{ij}$. Thus in the 4th term above

$$\begin{aligned} \breve{\boldsymbol{\tau}} : \boldsymbol{\nabla}\underline{\boldsymbol{u}} &= 0\,, \\ \boldsymbol{\nabla} \cdot \left(\breve{\boldsymbol{\tau}} \cdot \underline{\boldsymbol{u}}\right) &= (\boldsymbol{\nabla} \cdot \breve{\boldsymbol{\tau}}) \cdot \underline{\boldsymbol{u}} + \breve{\boldsymbol{\tau}} : \boldsymbol{\nabla}\underline{\boldsymbol{u}} = (\boldsymbol{\nabla} \cdot \breve{\boldsymbol{\tau}}) \cdot \underline{\boldsymbol{u}}\,. \end{aligned} \tag{37}$$

In the second term above, an inner product must be formed, and we note that $(\underline{\boldsymbol{v}} \otimes \underline{\boldsymbol{v}}) : \boldsymbol{\nabla}\underline{\boldsymbol{u}} = 0$. From the definitions of scalar, outer and inner products and the inter-frame velocity $\underline{\boldsymbol{u}}$, a number of vector relations arise, in addition to which

$$\boldsymbol{\nabla} \cdot \left(p\underline{\boldsymbol{u}}\right) = (\boldsymbol{\nabla}p) \cdot \underline{\boldsymbol{u}} = [\boldsymbol{\nabla} \cdot (p\boldsymbol{I})] \cdot \underline{\boldsymbol{u}} \tag{38}$$

and

$$\boldsymbol{\nabla} \cdot \left[\underline{\boldsymbol{v}}\left(\breve{\boldsymbol{v}} \cdot \underline{\boldsymbol{u}}\right)\right] = [\boldsymbol{\nabla} \cdot \left(\underline{\boldsymbol{v}} \otimes \breve{\boldsymbol{v}}\right)] \cdot \underline{\boldsymbol{u}} + (\breve{\boldsymbol{\omega}} \times \underline{\boldsymbol{v}}) \cdot \underline{\boldsymbol{u}}. \tag{39}$$

Now (36) can be expressed in terms of velocities defined in the relative frame $\underline{\boldsymbol{v}}$ and $\underline{\boldsymbol{u}}$:

$$\begin{aligned} &\frac{\partial}{\partial t}\left(\rho\breve{\boldsymbol{v}} \cdot \underline{\boldsymbol{u}}\right) + \left\{\boldsymbol{\nabla} \cdot \left[\rho\underline{\boldsymbol{v}} \otimes \breve{\boldsymbol{v}} + p\boldsymbol{I} - \breve{\boldsymbol{\tau}}\right]\right\} \cdot \underline{\boldsymbol{u}} \\ &\qquad = -\rho(\breve{\boldsymbol{\omega}} \times \breve{\boldsymbol{v}}) \cdot \underline{\boldsymbol{u}} + \rho\breve{\boldsymbol{v}} \cdot \dot{\underline{\boldsymbol{u}}} + \rho\breve{\boldsymbol{g}} \cdot \underline{\boldsymbol{u}} \frac{\partial}{\partial t}\left(\rho\breve{\boldsymbol{v}} \cdot \underline{\boldsymbol{u}}\right) \\ &+ [\boldsymbol{\nabla} \cdot \left(\rho\underline{\boldsymbol{v}} \otimes \breve{\boldsymbol{v}}\right)] \cdot \underline{\boldsymbol{u}} + \boldsymbol{\nabla} \cdot (p\underline{\boldsymbol{u}}) - \boldsymbol{\nabla} \cdot (\breve{\boldsymbol{\tau}} \cdot \underline{\boldsymbol{u}}) - \rho(\breve{\boldsymbol{\omega}} \times \breve{\boldsymbol{v}}) \cdot \underline{\boldsymbol{u}} + \rho\breve{\boldsymbol{v}} \cdot \dot{\underline{\boldsymbol{u}}} + \rho\breve{\boldsymbol{g}} \cdot \underline{\boldsymbol{u}} \end{aligned} \tag{40}$$

Using (3)

$$\frac{\partial}{\partial t}\left(\rho\breve{\boldsymbol{v}} \cdot \underline{\boldsymbol{u}}\right) + \boldsymbol{\nabla} \cdot [\rho\underline{\boldsymbol{v}}\left(\breve{\boldsymbol{v}} \cdot \underline{\boldsymbol{u}}\right) + p\underline{\boldsymbol{u}} - \breve{\boldsymbol{\tau}} \cdot \underline{\boldsymbol{u}}] = \rho\breve{\boldsymbol{v}} \cdot \dot{\underline{\boldsymbol{u}}} + \rho\breve{\boldsymbol{g}} \cdot \underline{\boldsymbol{u}} \tag{41}$$

By subtraction of equation (41) from the differential form of equation (32),

$$\begin{aligned} &\frac{\boldsymbol{\partial}}{\boldsymbol{\partial t}}\boldsymbol{\rho}\left(\boldsymbol{E} - \breve{\boldsymbol{v}} \cdot \underline{\boldsymbol{u}}\right) + \boldsymbol{\nabla} \cdot [\boldsymbol{\rho}\underline{\boldsymbol{v}}\left(\boldsymbol{E} - \breve{\boldsymbol{v}} \cdot \underline{\boldsymbol{u}}\right) + \boldsymbol{p}\underline{\boldsymbol{v}} - \breve{\boldsymbol{\tau}} \cdot \underline{\boldsymbol{v}} - \boldsymbol{\kappa}\boldsymbol{\nabla}\boldsymbol{T}] \\ &\qquad = q_H + \rho\underline{\boldsymbol{v}} \cdot \breve{\boldsymbol{g}} - \rho\breve{\boldsymbol{v}} \cdot \dot{\underline{\boldsymbol{u}}} \end{aligned} \tag{42}$$

It is now convenient to introduce a generalized rothalpy E* defined by

$$E^* = E - \breve{\boldsymbol{v}} \cdot \underline{\boldsymbol{u}} = e + \tfrac{\|\boldsymbol{u}\|^2 + \|\boldsymbol{v}\|^2}{2} \tag{43}$$

so that

$$\tfrac{\partial}{\partial t}\rho E^* + \boldsymbol{\nabla} \cdot \left[\rho\underline{\boldsymbol{v}}E^* + p\underline{\boldsymbol{v}} - \breve{\boldsymbol{\tau}} \cdot \underline{\boldsymbol{v}} - \kappa\boldsymbol{\nabla}T\right] = q_H + \rho\underline{\boldsymbol{v}} \cdot \breve{\boldsymbol{g}} - \rho\left(\underline{\boldsymbol{v}} + \underline{\boldsymbol{u}}\right) \cdot \dot{\underline{\boldsymbol{u}}} \tag{44}$$

or

$$\begin{aligned} &\frac{\partial}{\partial t}\int_V \rho E^* dV + \oint_{\partial V} \left(\rho E^* \underline{\boldsymbol{v}} + p\underline{\boldsymbol{v}} - \breve{\boldsymbol{\tau}} \cdot \underline{\boldsymbol{v}} - \kappa\boldsymbol{\nabla}T\right) \cdot d\underline{\boldsymbol{S}} \\ &\qquad = \int_V \left(q_H + \rho\underline{\boldsymbol{v}} \cdot \breve{\boldsymbol{g}} - \rho\left(\underline{\boldsymbol{v}} + \underline{\boldsymbol{u}}\right) \cdot \dot{\underline{\boldsymbol{u}}}\right) dV. \end{aligned} \tag{45}$$

This is an equation for energy conservation written in terms of generalized rothalpy and relative frame velocities. Written instead in terms of velocities in Σ', the rotation or spin $\breve{\boldsymbol{\omega}}$, and the dynamics of O' with respect to O denoted by $\ddot{\breve{\boldsymbol{r}}}$ and $\dot{\boldsymbol{r}}$, the equation is

$$\frac{\partial}{\partial t}\rho E^* + \boldsymbol{\nabla}\cdot\left[\rho\underline{\boldsymbol{v}}E^* + p\underline{\boldsymbol{v}} - \breve{\boldsymbol{\tau}}\cdot\underline{\boldsymbol{v}} - \kappa\boldsymbol{\nabla}T\right]$$
$$= q_H + \rho\underline{\boldsymbol{v}}\cdot\breve{\boldsymbol{g}} - \rho\left(\underline{\boldsymbol{v}} + \underline{\boldsymbol{u}}\right)\cdot\dot{\breve{\boldsymbol{r}}} - \rho\left(\underline{\boldsymbol{v}} + \underline{\boldsymbol{u}}\right)\cdot\left(\dot{\breve{\boldsymbol{\omega}}}\times\underline{\boldsymbol{x}}\right) \tag{46}$$
$$= q_H + \rho\underline{\boldsymbol{v}}\cdot\breve{\boldsymbol{g}} - \rho\underline{\boldsymbol{v}}\cdot\dot{\breve{\boldsymbol{r}}} - \rho\breve{\boldsymbol{r}}\cdot\dot{\breve{\boldsymbol{r}}} - \rho\left(\breve{\boldsymbol{\omega}}\times\underline{\boldsymbol{x}}\right)\cdot\dot{\breve{\boldsymbol{r}}} - \rho\underline{\boldsymbol{v}}\cdot\left(\dot{\breve{\boldsymbol{\omega}}}\times\underline{\boldsymbol{x}}\right)$$
$$- \rho\breve{\boldsymbol{r}}\cdot\left(\dot{\breve{\boldsymbol{\omega}}}\times\underline{\boldsymbol{x}}\right) - \rho\left(\breve{\boldsymbol{\omega}}\times\underline{\boldsymbol{x}}\right)\cdot\left(\dot{\breve{\boldsymbol{\omega}}}\times\underline{\boldsymbol{x}}\right)$$

The source terms may be interpreted as, from left to right from the second term, as the work associated with: the gravity body force as seen in Σ'; the acceleration $O'$with respect to O, of the fluid in the element, with velocity $\underline{\boldsymbol{v}}$ seen in Σ'; the acceleration of $O'$with respect to O at the velocity of $O'$with respect to O; the acceleration of $O'$with respect to O at the spin velocity seen in Σ'; the Euler acceleration due to spin-up or spin-down on the fluid in the element with velocity $\underline{\boldsymbol{v}}$; the velocity of $O'$with respect to O and the Euler acceleration; and the Euler acceleration on the spin velocity seen in Σ'. The Coriolis effect has correctly disappeared from equation (46).

3.7 Constitutive relations

In the equations of state of the gas, ρ, p and T transform as invariants. The constitutive relation for the viscous stress tensor can be expressed in Σ as follows:

$$\boldsymbol{\tau} = \lambda(\boldsymbol{\nabla}\cdot\boldsymbol{v})\boldsymbol{I} + 2\mu[(\boldsymbol{\nabla}\boldsymbol{v}) + (\boldsymbol{\nabla}\boldsymbol{v})^T], \tag{47}$$

where λ is the bulk viscosity and μ is the dynamic viscosity. Both λ and μ may be treated as functions of ρ, p and T, which are invariant. As a second order tensor, τ is transformed by equation (6). The first term becomes

$$\breve{\boldsymbol{\tau}}_1 = \boldsymbol{U}^t\cdot\lambda(\boldsymbol{\nabla}\cdot\boldsymbol{v})\boldsymbol{I}\cdot\boldsymbol{U}. \tag{48}$$

Using the scalar product definition in section 3.5, the inverse mapping φ^* in section 3.3, and the definition of $\boldsymbol{\nabla}\cdot\boldsymbol{\Theta}$ in section 3.5, it can be seen that $\varphi^*\left(\boldsymbol{\nabla}\cdot\boldsymbol{v}\right) = \boldsymbol{\nabla}\cdot[\boldsymbol{U}^t\cdot(\varphi^*\boldsymbol{v})]$**,** and

$$\breve{\boldsymbol{\tau}}_1 = \breve{\lambda}(\boldsymbol{\nabla}\cdot\breve{\boldsymbol{v}})\boldsymbol{I} \tag{49}$$

where $\breve{\lambda} = \boldsymbol{\phi}^*\lambda$ (section 3.3) and the spatial derivative is in Σ'. With the definition of interframe velocity in equation (12), $\boldsymbol{\nabla}\cdot\underline{\boldsymbol{u}} = 0$, and

$$\breve{\boldsymbol{\tau}}_1 = \breve{\lambda}\left(\boldsymbol{\nabla}\cdot\underline{\boldsymbol{v}}\right)\boldsymbol{I}. \tag{50}$$

Similarly, the grad operator transforms as

$$\varphi^*\left(\boldsymbol{\nabla}_{\boldsymbol{x}}\boldsymbol{v}\right) = \boldsymbol{\nabla}_{\breve{\boldsymbol{x}}}(\varphi^*\boldsymbol{v}).$$

The second term becomes

$$\breve{\boldsymbol{\tau}}_2 = 2\breve{\mu}\,\boldsymbol{U}^t\cdot[(\boldsymbol{\nabla}\boldsymbol{v}) + (\boldsymbol{\nabla}\boldsymbol{v})^T]\cdot\boldsymbol{U}, \tag{51}$$

and with the spatial derivatives written in Σ'

$$\breve{\boldsymbol{\tau}}_2 = 2\breve{\mu}[(\boldsymbol{\nabla}\breve{\boldsymbol{v}}) + (\boldsymbol{\nabla}\breve{\boldsymbol{v}})^T]. \tag{52}$$

For $\underline{\boldsymbol{u}}$ defined by equations (11) and (12) as the sum of a translation and a rotation, it is easily shown that $\boldsymbol{\nabla}\cdot\underline{\boldsymbol{u}} = 0$ and that $\boldsymbol{\nabla}\underline{\boldsymbol{u}}$ is antisymmetric. In writing $\boldsymbol{\nabla}\breve{\boldsymbol{v}}$ in terms of $\boldsymbol{\nabla}\underline{\boldsymbol{v}}$**,** therefore, interframe velocity gradients vanish, and

$$\breve{\boldsymbol{\tau}} = \breve{\lambda}\left(\boldsymbol{\nabla}\cdot\underline{\boldsymbol{v}}\right)\boldsymbol{I} + 2\breve{\mu}\left[\left(\boldsymbol{\nabla}\underline{\boldsymbol{v}}\right) + \left(\boldsymbol{\nabla}\underline{\boldsymbol{v}}\right)^T\right]. \tag{53}$$

For problems in which relaxation times for local flow are important, it is useful to refer to an analysis by de Groot and Mazur [62] in which pure rotation of a fluid is considered. In the inertial frame, angular momentum is decomposed into a spin component (local rotation of fluid elements, as described by $\boldsymbol{U}$ in the present work) and a component describing bulk revolution about a centre of rotation (as described by $\boldsymbol{r}$ in the present work, in which completely arbitrary motion is of interest). In the pure rotation case, de Groot and Mazur defined a rotational viscosity which can be related to a relaxation time purely for local fluid element spin.

3.8 Conservation summary

The analysis in the sections above has been performed for several purposes. A point that is illustrated is that for simulation of compressible flow in the relative frame, each source term added in coding must be separately verified and validated in a numerical model constructed for the purpose.

Equations (21), (26), and (45) form a statement of the conservation laws in integral form, and equations (22), (27) and (46) are the equivalent statements in differential form. Equation (53) gives the

transformed viscous stress tensor. In specific cases, dimensionless numbers can be devised to assist in estimating the dominance of effects observed in the relative frame on a case-by-case basis.

4 Dimensionless numbers

The effects described above have been considered negligible in most cases of aeronautical interest. It may however be necessary to determine the magnitude of these effects for missiles undergoing "significant" acceleration. Several approaches can be followed to determine what accelerations are "significant". Of these, the simplest, and most approximate, is to determine the relative size of terms in the equations of motion, and to understand regimes in which various effects are expected. This has been done to a large extent for fluid phenomena in the circulation of the earth's atmosphere, leading to the formulation of the Rossby number and the investigation of Taylor-Proudman vortices in incompressible flow within closed boundaries [5,6].

The approach of devising dimensionless numbers is useful in determining flow regimes, but is essentially a linear approximation. Insofar as the approach can be used in any general way, rather than in specific cases, the method is shown for the momentum equation here, and can be adapted to the energy equation as well.

Following Boubnov and Golitsyn [8], a change of variables is made with respect to typical scales as follows:

$$\begin{aligned} &\varphi = \varphi_0 \varphi^*,\ \boldsymbol{x} = L\boldsymbol{x}^*,\ \boldsymbol{\nabla} = \mathrm{L}^{-1}\boldsymbol{\nabla}^*, \\ \dot{\boldsymbol{\omega}} = \dot{\omega}_0 \dot{\boldsymbol{\omega}}^*, \qquad &\boldsymbol{v} = v_0 \boldsymbol{v}^*, \qquad \frac{\partial^2 \boldsymbol{r}}{\partial t^2} = a_0 \frac{\partial^2 \boldsymbol{r}^*}{\partial t^2} \ and \ \boldsymbol{\tau} = \nu \boldsymbol{\tau}^* \end{aligned} \tag{54}$$

where $\varphi = t, \omega, \rho, p, \boldsymbol{g}$ or $\boldsymbol{v}$, and where ν is a typical kinematic viscosity for the case, $\dot{\boldsymbol{\omega}}_0$ is a typical angular acceleration of spin about O', and a_0 describes linear acceleration of O' with respect to O, or revolution, or both. An example of revolution without rotation is that of an aerofoil with constant pitch attitude angle executing a circle about O, in which case the angle of attack varies during the revolution.

The scale factors are determined by the problem at hand. Rewriting the momentum equation (27) as the following, omitting the asterisks, and multiplying by $\frac{L}{\rho_0 {v_0}^2}$ in order to compare terms with convection gives

$$\begin{aligned} \frac{L}{v_0 t_0}\frac{\partial}{\partial t}(\rho \underline{\boldsymbol{v}}) + \boldsymbol{\nabla}\cdot\rho\underline{\boldsymbol{v}}\otimes\underline{\boldsymbol{v}} + \frac{p_0}{\rho_0 {v_0}^2}\nabla\cdot p\boldsymbol{I} - \frac{\nu}{\rho_0 {v_0}^2}\boldsymbol{\nabla}\cdot\breve{\boldsymbol{\tau}} \\ = -\frac{L^2{\omega_0}^2}{{v_0}^2}\rho\breve{\boldsymbol{\omega}}\times\left(\breve{\boldsymbol{\omega}}\times\underline{\boldsymbol{x}}\right) - 2\frac{L^2\omega_0}{{v_0}^2}\rho\breve{\boldsymbol{\omega}}\times\underline{\boldsymbol{v}} - \frac{L^2\dot{\omega}_0}{{v_0}^2}\rho\dot{\breve{\boldsymbol{\omega}}}\times\underline{\boldsymbol{x}} \\ -\frac{La}{{v_0}^2}\rho\ddot{\breve{\boldsymbol{r}}} + \frac{Lg_0}{{v_0}^2}\rho\breve{\boldsymbol{g}} \end{aligned} \tag{55}$$

Using the definitions of the Strouhal number, $St = \frac{v_0 t_0}{L}$; the Euler number, $Eu = \frac{\rho_0 {v_0}^2}{p_0}$; the Reynolds number, $Re = \frac{Lv_0}{\nu}$; the Rossby or Kibel number, $Ro = \frac{v_0}{2\omega_0 L}$; and the Froude number, $Fr = \frac{v_0}{\sqrt{Lg}}$, we can write

$$\begin{aligned} St^{-1}\frac{\partial}{\partial t}(\rho\underline{\boldsymbol{v}}) + \boldsymbol{\nabla}\cdot\rho\underline{\boldsymbol{v}}\otimes\underline{\boldsymbol{v}} + Eu^{-1}\nabla\cdot p\boldsymbol{I} - \frac{L}{v_0}Re^{-1}\boldsymbol{\nabla}\cdot\breve{\boldsymbol{\tau}} \\ = -\frac{L^2{\omega_0}^2}{{v_0}^2}\rho\breve{\boldsymbol{\omega}}\times\left(\breve{\boldsymbol{\omega}}\times\underline{\boldsymbol{x}}\right) - Ro^{-1}\rho\breve{\boldsymbol{\omega}}\times\underline{\boldsymbol{v}} - \frac{L^2\dot{\omega}_0}{{v_0}^2}\rho\dot{\breve{\boldsymbol{\omega}}}\times\underline{\boldsymbol{x}} - \frac{La_0}{{v_0}^2}\rho\ddot{\breve{\boldsymbol{r}}} + Fr^{-2}\rho\breve{\boldsymbol{g}} \end{aligned} \tag{56}$$

The first term and the Strouhal number characterize typical temporal behavior. The Euler term compares pressure and inertial effects. The Reynolds number arises from the comparison of viscous effect in translation (the normalization being different from the usual non-dimensionalisation leading to the Reynolds number), while in rotational viscous problems the Ekman number, $Ek = \frac{\nu}{L^2\omega_0} = 2Ro/Re$, arising from comparisons of the dominance of rotational and viscous effects, is used for example in understanding the development of viscous boundary layers on the walls of rotating vessels [9]; if rotation is near-rigid, then $L\omega_0 \approx v_0$ and the scale factors lead back to the Reynolds number.

The first source term is related to centrifugal effects viewed from the rotating frame Σ', and where a typical radius of rotation R applies for rigid body rotation the coefficient is of the order L^2/R^2

and the effect is easily visualised. The second term is the familiar Coriolis term characterised by the Rossby number. The third term is the spin-up or spin-down term. In the formulation provided here, ω_0 and $\dot{\omega}_0$ are linearly related by the typical time scale, but the time scale of angular acceleration can be decoupled from t_0 if this is appropriate for the problem. The final terms establish the equivalence of translational acceleration $a = \ddot{r}$ and gravity g in the relative motion of Σ' and Σ. We term the factor $Q = \frac{La_0}{{v_0}^2}$ the acceleration (or deceleration) parameter[1] and note that it is the counterpart of Fr^{-2}. It should be noted that $\boldsymbol{r}$ may describe revolution at a constant attitude angle, while $\boldsymbol{\omega}$ is spin and governs attitude changes. A set of parameters can now also be derived for the Euler acceleration and cross-coupling terms in equation (46) for specific circumstances.

Other dimensionless parameters for fluids still emerge from the Navier-Stokes equations and must be taken into account, most importantly including the Mach number M.

5 Illustrations

5.1 Linear acceleration

The works of Roohani and Skews [41,43,44] focus on acceleration and deceleration effects when the acceleration is parallel to the velocity of the object. In this case, the conservation equations in the relative frame Σ' are as follows, given that $\boldsymbol{\omega} = 0$, and therefore $\boldsymbol{U} = \boldsymbol{I}$. Conservation of mass remains

$$\frac{\partial \rho}{\partial t} + \boldsymbol{\nabla} \cdot (\rho \underline{\boldsymbol{v}}) = 0. \tag{57}$$

Conservation of momentum becomes, from (26) and (27)

$$\frac{\partial}{\partial t}(\rho \underline{\boldsymbol{v}}) + \boldsymbol{\nabla} \cdot \left[\rho \underline{\boldsymbol{v}} \otimes \underline{\boldsymbol{v}} + p\boldsymbol{I} - \breve{\boldsymbol{\tau}}\right] = -\rho \dddot{\breve{\boldsymbol{r}}} + \rho \breve{\boldsymbol{g}} \tag{58}$$

The equation for energy conservation written in terms of rothalpy and relative frame velocities in Σ' is now (45), (46)

$$\frac{\partial}{\partial t}\rho E^* + \boldsymbol{\nabla} \cdot \left[\rho \underline{\boldsymbol{v}} E^* + p\underline{\boldsymbol{v}} - \breve{\boldsymbol{\tau}} \cdot \underline{\boldsymbol{v}} - \kappa \boldsymbol{\nabla} T\right] = q_H + \rho \underline{\boldsymbol{v}} \cdot \breve{\boldsymbol{g}} - \rho \underline{\boldsymbol{v}} \cdot \ddot{\breve{\boldsymbol{r}}} + 2\rho \breve{\boldsymbol{r}} \cdot \ddot{\breve{\boldsymbol{r}}}. \tag{59}$$

With $\boldsymbol{\omega} = 0$, $\breve{\boldsymbol{g}} = \boldsymbol{g}$ by equations (2) and (5), and $\breve{\boldsymbol{r}} = \boldsymbol{r}$, $\ddot{\breve{\boldsymbol{r}}} = \ddot{\boldsymbol{r}}$ by (9) and (1). The acceleration parameter can be written as $Q = \frac{L\ddot{r}}{\dot{r}^2}$.

Roohani and Skews studied the effects of acceleration and deceleration on biconvex, diamond, NACA0012, NACA2412, and RAE2812 aerofoils. Parameters for their cases are shown in Table 1. For comparison, maximum thrust during the launch of a typical 90 *kg* Vth generation SRAAM (short range air-to-air missile) is or the order of 20 000 N. For present purposes we assume the altitude to be of the order of 30 000 feet and the Mach number in the region of 1.5.

Parameter	*Aerofoils, subsonic range*	*Aerofoils, transonic range*	*SRAAM, supersonic range*
Typical length L	1 m	1 m	3 m
Typical velocity v_0	100 ms^{-1}	300 ms^{-1}	464 ms^{-1}
Mach number M	0.3	1	1.5
Typical acceleration a_0	1041ms^{-2}	1041 ms^{-2}	980 ms^{-2}
Acceleration parameter $Q = \frac{La_0}{{v_0}^2}$	0.1	0.01	0.01
Freymuth start-up time $\sqrt{L/a}$	0.03 s	0.03 s	0.06s

Table 1 Typical parameters for aerofoils and air-to-air missiles. Data for aerofoils is from Roohani and Skews [44].

[1] For linear acceleration this is consistent with cosmological usage.

Significant effects on aerofoil lift and drag were observed [44] in the subsonic range, and we deduce that $Q{\sim}0.1$ may be a reasonable indicator in this range. In the high velocity ranges Q is lower, but shock wave effects dominate flow history in this range, as described under section 2, the Mach number M ~ 1. For supersonic missiles, studies using computational fluid dynamics remain to be done. The Freymuth start-up time is independent of velocity and should be shorter under more significant acceleration; together with the Mach number it provides a consistent predictor for the aerofoils.

The effects on drag are significantly different for acceleration, $\ddot{r}/\dot{r} > 0$, and deceleration $\ddot{r}/\dot{r} < 0$. This obviously important parameter determines whether wake effects and shocks propagate faster than the aerofoil itself. In this case, $\ddot{r}/\dot{r} < 0$, shocks may overtake an aerofoil [44], and stand-off bow shocks may exist at subsonic body velocities [44,52]. For transonic acceleration or $\ddot{r}/\dot{r} > 0$, shocks on convex surfaces are likely to be found forward of the steady state position [44]. In terms of flow history as defined above, this is due to persistent features of the flow field at an earlier time and a lower Mach number. Similarly, for deceleration or $\ddot{r}/\dot{r} < 0$, transonic shocks will be found aft of the steady state position on an airfoil surface and may be attached to the trailing edge at lower velocities than expected on steady-state grounds.

5.2 Flows confined by axisymmetric boundaries

The smooth, controlled combustion of fuel in solid rocket motors is a subject of considerable practical importance in trajectory predictability and control. A set of parameters describing the flow regimes may prove useful. A start may be made by considering parameters governing the development of Taylor-Proudman vortices in incompressible fluids in closed rotating containers [9]. While rocket motors are open containers, solid rocket charges are internally shaped, mass is variable, the fluids are compressible, and temperatures are such that real gas effects must be considered in flow, some insight may still be gained into the dominance of rotating effects by progressively working from simple assumptions such as rotation that may be almost rigid.

Taylor-Proudman vortices are possible when incompressibility and boundary conditions together make internal flow independent of the coordinate parallel to the rotational axis, which we will take to be z, and a perturbation along the axis will cause perturbation of streamlines independent of z [5,6] and will occur when rotational effects dominate, for example when $Ro \sim \frac{1}{2}$. Similar dynamics govern the establishment of rigid rotational flow near a spinning disk, for example a chamber end-wall, when the angular velocity is perturbed, or when the wall is moved along the rotational axis [9]. Viscous effects during spin-up or spin-down include the development of an Ekman layer in a plane normal to z and the propagation of a front between rotating and static flow towards, or away from, the axis [9] on time scales of the order of ${\omega_0}^{-1}$, and the establishment of rigid body flow on the typical time scale ${\omega_0}^{-1}\, Ek^{-1/2}$ (taking ν as that for dry air for approximate purposes).

Some data for rockets may be found in the literature from which the typical values have been deduced. Apache and Cajun sounding rockets were described by Uselton and Carman [63]; the radius was 59 mm and rotation rates were 1.5 to 32 rad s^{-1}. Marquardt *et al.* [64] provided data on highly manoeuvrable missiles, based on radius 59 mm and rotation rates of order 100 rad s^{-1}, but for which only limited information is available. Unguided fin-stabilised artillery rockets with 122 mm body diameter were covered by Khalil *et al*. [65] with typical muzzle spin rates of 100 rad s^{-1}.

	Low spin	***Medium spin***	***High spin***
Spin rate ω_0	1.5 $rad\ s^{-1}$	32 $rad\ s^{-1}$	100 $rad\ s^{-1}$
Radius *r*	59 mm	59 mm	61 mm
Ro, rigid	.5	.5	.5
Ek	$3.1\text{x}10^{-3}$	$1.4\text{x}10^{-4}$	$4.3\text{x}10^{-5}$
Ekman layer time	.67 s	.03 s	.01 s

$\omega_0{}^{-1}$			
Spin up time $\omega_0{}^{-1}\, Ek^{-1/2}$	12.0 s	2.6 s	1.5 s

Table 2 Internal flow parameters for the assumption of almost-rigid flow. Times are given by Greenspan [9]; parameters for low and medium spin conditions are sourced from Uselton and Carman [63] and for high spin conditions were given by Khalil *et al.* [65].

In the low spin and medium spin cases, if the chamber were to be considered to be closed and incompressible inviscid flow were to be assumed, Taylor-Proudman effects might be expected. In the high spin case, Taylor-Proudman effects might be expected and the Ekman layer would be established before burnout since the burn time is 1.8 s. If Taylor columns were to be established, the implication is that deformities in the grain would influence the flow field parallel to the spin axis along the length of the internal space. These are very considerable approximations. However, they illustrate the fact that some remarks may be made about rotational effects which may affect grain burn under certain circumstances.

While the examples above illustrate well-known parameters, the aim in introducing them here is to add to the basis on which useful parameters for arbitrary manoeuvre can be built.

6 CFD implementation

A few relevant studies have already been undertaken with Computational Fluid Dynamics models and in the following paragraphs the methodologies of different implementations are discussed. ANSYS FLUENT and STAR-CCM+ are two commercial CFD software packages, allowing the use of multiple solvers, compressibility models, moving mesh capabilities and a large range of turbulence models. They are both useful in investigations into the unsteady aerodynamics of accelerating bodies. However, the approach that is used with each code is completely different.

STAR-CCM+ is of interest because of its use of overset meshing, also known as Chimera meshing [66,67]. This is a capability where a mesh overlaps, or is superimposed on, another mesh in the computational domain. The two meshes are coupled and a reference system is incorporated to interpolate the values of the cell variables of each mesh through the use of algebraic equations. This meshing option is most commonly implemented in cases with moving bodies. The background mesh representing the fluid is held stationary and the overset mesh moves with the moving body, thus providing an inertial reference frame. The velocity of the overset mesh can either be characterized by a user defined function or by a set of tabulated values. One drawback of this approach is that for large unidirectional velocities a very large background domain is required resulting in excessive computational time. However, it is well suited to problems analysing combined rotational and translational acceleration over short distances.

ANSYS FLUENT [46] uses a non-inertial reference frame where a single mesh system is used. In order to model an accelerating body the object is held stationary and the fluid in every cell in the meshed domain is accelerated simultaneously with equal acceleration across the domain. User defined functions are required in order to define the acceleration at the boundary of the domain and to add source terms to the momentum and energy equations to ensure that the same acceleration is implemented within the meshed domain. This approach is useful for analysing problems with large unidirectional velocities and accelerations as the size of the meshed domain remains fixed resulting in reduced computational time compared to inertial reference frame systems.

A different approach to implementation has been taken within the codes EURANUS [68] and its successor Edge [31]. Edge is an unstructured dual-grid compressible flow solver on arbitrary elements based on a node-centred finite volume technique. The code was designed for aeroelastic application and is based on moving grids, and this greatly simplifies the adaption of the code to providing a rigid moving grid directly implemented in the absolute frame Σ. No source terms are needed, or need to be verified, in this implementation. Simulations in this frame have been tested and validated [1]. The major advantage of rigid-grid absolute frame CFD is that the domain is the size of a traditional CFD grid for a missile, extending only to far field boundaries of the order of 20 typical lengths away from the object. It was necessary to provide the basic transforms, equations (7) and (9), for use with results, since most velocity flow fields in the absolute frame appear unfamiliar.

Arbitrary Lagrangian-Eulerian (ALE) methods are based on a third frame of reference which may, or may not, be coincident with the Lagrangian or Eulerian frame [69], and have proved useful in finite-element models of deforming materials, free surfaces, and fluid-structure interactions [70]. While they have been applied to prediction of dynamic derivatives [71], instances of the use of ALE models for long trajectory manoeuvre or acceleration have not been encountered.

7 Discussion

The purposes and results of writing the conservation equations in the forms above are as follows.

The general transform is needed for the interpretation of CFD results. Conventionally, CFD has been performed in the relative frame, and results are inspected in this frame in a familiar form. If computation is performed in the absolute frame using a moving grid, and then displayed on that grid, $\boldsymbol{v} = 0$ at the boundaries in stagnant air in Σ while $\boldsymbol{v} \neq 0$ at stagnation points (defined as points at which the flow velocity equals the wall velocity). Potential confusion can be overcome by inspecting flow fields in both frames.

This set of equations allows the identification of flow dynamics and features in both frames. For example, Gledhill *et al*. [1] shows that missile strake vortex cores deflect from their steady-state paths towards the turn centre in a constant-pitch turn and may disrupt expected fin dynamics. In the relative frame this can be interpreted as a centrifugal effect, displacing higher-density fluid away from the turn centre. Similarly, awareness of the well-known dynamics of rotating flow may assist in building an understanding of flow under accelerated conditions as illustrated by the spinning rocket examples above.

The Navier-Stokes equations have been displayed in a form that lends itself to finite volume implementation in CFD, in both absolute and relative frames. The source terms are explicitly listed and interpreted for the relative frame. The effects of each source term implemented need to be verified and validated.

A full set of dimensionless numbers has been collected for the momentum equation applied to arbitrary manoeuvre in order to guide estimation of regimes in which significant acceleration effects may appear. The Mach number is an important addition to this set. Examples of significant effects have been illustrated through published results for linearly accelerating and decelerating aerofoils, and it is predicted that air-to-air missiles are within the acceleration range at launch at which effects are significant.

In unidirectional linear acceleration, the acceleration parameter $Q = La_0/{v_0}^2$ is derived directly from the momentum equation in the relative frame. This parameter does not take compressible effects into account but does indicate the size of linear acceleration terms in comparison with convection. The obvious importance of acceleration or deceleration, $\ddot{r}/\dot{r}$, has been illustrated with reference to the models of Roohani and Skews [45] and the experiments and simulations of Saito *et al.* [52].

A few examples of dimensionless parameters in very simplified configurations have been given. For angular acceleration or for constant angular velocity, these equations reduce to those in the literature of rotating flow, and the case of the Taylor-Proudman theorem follows.

Turbulence models have been developed over the years based on observations in constant velocity wind tunnel cases, and can therefore be regarded as holding in the inertial frame. Using the formulation developed here, the equations for turbulence models can easily be transformed into a non-inertial frame, but the question of how turbulence behaves for rapidly accelerating objects has yet to be investigated and answered.

8 Conclusions

This paper has presented the formulation of continuity, momentum, and energy equations for fluids in a way that enables manipulation of these equations across absolute inertial and body-fixed relative frames for arbitrary acceleration.

These expressions are now in a form that allows selected terms to be transformed clearly between non-inertial and inertial frames, and explicitly shows the coordinate system in which each vector or tensor is expressed. The transforms allow CFD results to be shown in the relative frame, which is the frame traditionally used in CFD and therefore often used for flow field interpretation, and the absolute frame, in which computation is simpler but results are less intuitively easy to construe. Both gravity and linear acceleration are formally included.

The derivation of a number of dimensional constants has been demonstrated in order to provide some guidance on regimes in which accelerating flow would be expected to be significant.

Acknowledgements

This document is partially a result of a research effort funded by the DRDB in terms of Armscor Orders KT466921, KT528944 and KT470887 before 2006. I. Gledhill wishes to acknowledge with gratitude the joint project set up by the CSIR that made this work possible, and the great hospitality of the University of the Witwatersrand School of Mechanical, Industrial and Aeronautical Engineering without which it could not have been completed. H. Roohani acknowledges the contribution of the Fluent and CD-adapco teams in accomplishing the simulations.

References

[1] Gledhill, I.M.A., Forsberg, K., Eliasson, P., Baloyi, J., Nordström, J.: Investigation of acceleration effects on missile aerodynamics using computational fluid dynamics. Aerosp. Sci. Tech. **13**(4), 197–203 (2009)
[2] Landau, L. D., Lifshitz, E. M.: Fluid Mechanics. Pergamon Press (1959)
[3] Batchelor, G.K.: An Introduction to Fluid Dynamics. Camb. Univ. Press (1967)
[4] Hough, S.S.: On the application of harmonic analysis to the dynamical theory of the tides. Part I. Philos. Trans. R. Soc. Lond. A **189**, 201–257 (1897)
[5] Proudman, J.: On the motion of solids in liquids possessing vorticity. Proc. R. Soc. Lond. **92**, 408–424 (1916)
[6] Taylor, G.I.: Motion of solids in fluids when the flow is not irrotational. Proc. R. Soc. Lond. A **93**,92–113 (1917)
[7] Taylor, G.I.: Experiments with rotating fluids. Proc. R. Soc. Lond. A **100**, 114–121 (1921)
[8] Boubnov, B. M., Golitsyn, G.S.: Convection in Rotating Fluids. Springer Science+Business (1995)
[9] Greenspan, H.P.: The Theory of Rotating Fluids. Camb. Univ. Press, Cambridge (1990)
[10] Owczarek, J.A.: Fundamentals of Gas Dynamics. Int. Textb. Co., Scranton, Pennsylvania (1964)
[11] Parmar, M., Haselbacher, A., Balachandar, S.: Generalized Basset-Boussinesq-Oseen equation for unsteady forces on a sphere in a compressible flow. Phys. Rev. Lett. **106**, 084501 (2011)
[12] Basset, B.A.: Treatise on Hydrodynamics. Deighton, Bell and Co., Cambridge (1888)
[13] Blasius, H.: Grenzschichten in Flüssigkeiten mit kleiner Reibung. Z. Math. Phys. **56**, 1–37 (1908). English translation in NACA-TM-1256
[14] Görtler, H.: Verdrängungswirkung der laminaren grenzschicht und druckwiderstand. Ing.-Arch. **14**, 286–305 (1944)
[15] Schlichting. H.: Boundary Layer Theory. Springer, 8th edition (2000)
[16] Sozou, C.: Boundary layer growth on a spinning sphere. J. Inst. Math. Appl., **7**, 251–259 (1971)
[17] Z. Zapryanov. Boundary layer growth on a spinning sphere. ZAMM. Z. angew. Math. Mech. **57**, 41–46 (1977)
[18] Guo, J.: Motion of spheres falling through fluids. J. Hydraul. R. **49**, 32–41 (2011)
[19] Launder, B.E., Jones, W.P.: Sink flow turbulent boundary layers. J. Fluid Mech. **38**, 817–831 (1969)
[20] Coles, D.E., Hirst, E.A.: Computation of turbulent boundary layers. In 1968 AFOSR-IFP-Stanford Conference, Vol. II. Stanford Univ., CA (1969)
[21] Piomelli, U., Yuan, J.: Numerical simulations of spatially developing, accelerating boundary layers. Phys. Fluids **25**, 101304 (2013)
[22] Lilley, G.M., Westley R., Yates, A.H., Busing, J.R.: Some aspects of noise from supersonic aircraft. J. R. Aeronaut. Soc. College of Aeronautics Report *71*, 57:396–414, 1953.
[23] Olver, P.J.: Moving frames. J. Symb. Comput. **36**, 501–512 (2003)
[24] Poludnenko, A.Y., Khokholov, A.M.: Computational of fluid flows in non-inertial contracting, expanding, and rotating reference frames. J. Comput. Phys. **220**, 678–711 (2007)
[25] Chhay, M., Hamdouni, A.: A new construction for invariant numerical schemes using moving frames. C. R. Mec. **338**, 97–101 (2010)
[26] Rahman, M., Bhatta, D.D.: Evaluation of added mass and damping coefficient of an oscillating circular cylinder. Appl. Math. Model. **17**, 70–79 (1993)

[27] Fackrell, S.: Study of the added mass of cylinders and spheres. PhD thesis, Univ. of Windsor (2011)
[28] Sosnowski, S. , Franosch, J.M.P., Zhang, L., Nie, Y., Kühnlenz, K., Hirche, S., and van Hemmen, J. L.: Simulation of the underwater vehicle "Snookie": Navigating like a fish. In 1st Int. Conference on Applied Bionics and Biomechanics (2010)
[29] Freymuth, P., Bank, W., Palmer, M.: Visualization of accelerating flow around an airfoil at high angles of attack. Z. Flugwiss. Weltraumforsch. **7**, 392–400 (1983)
[30] Forsberg, K., Gledhill, I.M.A., Eliasson, P., Nordström, J.: Investigations of acceleration effects on missile aerodynamics using CFD. AIAA-2003-4084 (2003)
[31] Eliasson, P., Nordström, J.: The development of an unsteady solver for moving meshes. Tech. Rep., Flygtekniska Försöksanstalten, The Swedish Aeronautical Institute, FFA-TN 1995-39 (1995)
[32] Limache, A. C., Cliff,E. M. Aerodynamic sensitivity theory for rotary stability derivatives. J. Aircr. 37:676–683, 2000.
[33] Limache, A.C. Aerodynamics modeling using Computational Fluid Dynamics and sensitivity equations. PhD thesis, Virginia Polytechnic Institute and State University, Blacksburg, VA, 2000.
[34] Kageyama, A., Hyodo, M.: Eulerian derivation of the Coriolis force. Geochem. Geophys. Geosyst. **7**, Q02009 (2006)
[35] Gardi, A.G.: Moving reference frame and Arbitrary Lagrangian Eulerian approaches for the study of moving domains in Typhon. Master's thesis, Politecnico di Milano (2011)
[36] Combrinck, M.L., Dala, L.N. Eulerian derivations of non-inertial Navier-Stokes equations. In 29th Congr. Int. Counc. Aeronaut. Sci. 0577, 2014.
[37] Inoue, O., Sakai, T., Nishida, M.: Focussing shock waves generated by an accelerating projectile. Fluid Dyn. R. **21**,413–416 (1997)
[38] Landon, R.H.: NACA 0012 oscillating and transient pitching, Compendium of Unsteady Aerodynamic Measurements, Data Set 3, AGARD-R-702. Tech. Rep., AGARD (1982)
[39] Gledhill, I.M.A., Baloyi, J., Maserumule, M., Forsberg, K., Eliasson, P., Nordström, J.: Accelerating systems: some remarks on pitch damping. In: 5th S. Afr. Conf. Comput. Appl. Mech., Cape Town, pp. 268–275 (2006)
[40] Roohani, H., Skews, B.W.: Transient aerodynamic forces experienced by aerofoils in accelerated motion. In: 26th Int. Symp. on Shock Waves, A3550 (2007)
[41] Roohani, H., Skews, B.W.: Effect of acceleration on shock-wave dynamics of aerofoils during transonic flight. In 26th Int. Symp. on Shock Waves A3351 (2007)
[42] Roohani, H., Skews, B.W.: Shock wave profiles on a transonic wing during acceleration. In 27th Int. Symp. on Shock Waves (2008)
[43] Roohani, H., Skews, B.W.: Unsteady aerodynamic effects experienced by aerofoils during acceleration and retardation. Proc. Inst. Mech. Eng. **222**, 631–305 (2008)
[44] Roohani, H., Skews, B.W.: The influence of acceleration and deceleration on shock wave movement on and around airfoils in transonic flight. Shock Waves. **19**, 297–305 (2009)
[45] Roohani, H., Skews, B.W.: The aerodynamic effects of acceleration and retardation on axisymmetric bodies. In: 6th S. Afr. Conf. Comput. Appl. Mech., Mechanics SACAM08 (2008)
[46] Fluent 13.0 User's Guide. ANSYS® Inc. (2010)
[47] Roohani, H.: Aerodynamic effects of accelerating objects in air. PhD Thesis, Univ. of the Witwatersrand, Johannesburg (2010)
[48] Naidoo, K., Skews, B.W.: Dynamic effects on the transition between regular and Mach reflection of shock waves: new numerical and experimental results. J. Fluid Mech. **676**, 432–460 (2011)
[49] Naidoo , K., Skews, B.W.: Dynamic transition from Mach to regular reflection of shock waves in steady flow. J. Fluid Mech. **750**, 385–400 (2014)
[50] Weinacht, P., Sturek, W.B., Schiff, L.B.: Navier-Stokes prediction of pitch damping for axisymmetric projectiles. J. Spacecr. Rocket. **3**4, 753–761 (1997)
[51] Weinacht, P.: Navier-Stokes prediction of the individual components of the pitch-damping sum. J. Spacecr. Rocket. **35**, 598–605 (1998)
[52] Saito, T., Hatanaka, K., Yamashita, H., Ogawa, T., Obayashi, S., Takayama, K.: Shock stand-off distance of a solid sphere decelerating in transonic velocity range. Shock Waves. **21**, 483–489 (2011)
[53] Weinacht, P., Sturek, W.B.: Computation of the roll characteristics of finned projectiles. Tech. Rep., US Army Laboratory Command Tech. Rep. BRL-TR-2931 (1988)

[54] Cornier, J., Champagneux, S., Moreuxt, V., Collercandy, R.: Prediction of quasistationary aerodynamic coefficients using the ALE method. In: ECCOMAS 2000, Barcelona, Spain (2000)
[55] Murman, S.M.: A reduced-frequency approach for calculating dynamic derivatives. AIAA-2005-0840 (2005)
[56] Sturek, W.B., Nietubicz, C.J., Sahu, J., Weinacht, P.: Applications of computational fluid-dynamics to the aerodynamics of projectiles. J. Spacecr. Rocket. **31,** 186–199 (1994)
[57] Murman, S.M., Aftosmis, S.J., Berger, M.J.: Numerical simulation of rolling airframes using a multi-level Cartesian method. AIAA-2002-2798 (2002)
[58] McIlwain, S.T., Mallon, P.C.G., Fleming, R.J., McConnell, G.: An experimental and numerical study of a supersonic spinning missile. In North Atlantic Treaty Organization (NATO) Research Technology Organization Missile Aerodynamics RTO-MP-5 AC/323(AVT)TP/3 (1998)
[59] Costello, M., Sahu, J.: Using computational fluid dynamic/rigid body dynamic results to generate aerodynamic models for projectile flight simulation. Proc. Inst. Mech. Eng. Part G: J. Aerospace Engineering. **222**, 1067–1079 (2008)
[60] Da Ronch, A., Ghoreyshi, M., Badcock, K.J.: On the generation of flight dynamics aerodynamic tables by computational fluid dynamics. Prog. Aerosp. Sci. **47**, 597–620 (2011)
[61] Ghoreyshi, M., Jiràsek, A., Cummings, R.M.: Computational investigation into the use of response functions for aerodynamic-load modeling. AIAA J. **50**, 1314–1327 (2012)
[62] de Groot, S.R., Mazur, P.: Non-equilibrium thermodynamics. N.-Holl. Publ. Co., Amsterdam, (1984)
[63] Uselton, J.C., Carman, J.B.: Wind tunnel tests on the Apache sounding rocket with various spin rates at supersonic speeds. Tech. Rep., Defense Tech. Inf. Cent. DTIC Doc. AEDC-TR-69-57 (1969)
[64] Marquart, E.J., Lawrence, W.R., Lawrence, F.C.: Missile aerodynamic testing at the Arnold Engineering Development Cent. In North Atlantic Treaty Organization (NATO) Research Technology Organization Missile Aerodynamics RTO-MP-5 AC/323(AVT)TP/3 (1998)
[65] Khalil, M., Abdalla, H., Kamal, O.: Trajectory prediction for a typical fin stabilized artillery rocket. In: 13th Int. Conf. Aerosp. Sci. Aviat. Tech. ASAT- 13 (2009)
[66] CD-adapco User Guide STAR-CCM+ Version 7.02.008, CD-adapco (2012)
[67] Steger, J.L., Dougherty, F.C., Benek, J.A.: A Chimera grid scheme. In: Advances in Grid Generation; Proceedings of the Applied Mechanics, Bioengineering, and Fluids Engineering Conference A84-11576 02-64, Am. Soc. Mech. Eng. (1983)
[68] Eliasson, P., Nordström, J., Torngren, L., Tysell, L., Karlsson, A., Winzell, B.: Computations and measurements of unsteady pressure on a delta wing with an oscillating flap. In: Proc. 3rd ECCOMAS CFD Conf. Wiley, Paris (1996)
[69] Hirt, C.W, Amsden, A.A, Amsden, J.L.: An arbitrary Lagrangian-Eulerian computing method for all flow speeds. J. Comput. Phys. **14**, 227 – 253 (1974)
[70] Donea, J., Giuliani, S., Halleux, J.P.: An arbitrary Lagrangian-Eulerian finite element method for transient dynamic fluid-structure interactions. Comput. Methods Appl. Mech. Eng. **33**, 689–723 (1982)
[71] Oktay, E., Akay, H.U., Uzun, A.: Parallelized three-dimensional unstructured Euler solver for unsteady aerodynamics. J. Aircr. **40**, 348–354 (2003)